

# TECHNICAL DEVELOPMENT REPORT

## EFFECT OF COPPER ON THE CORROSION RESISTANCE BEHAVIOUR OF AS-CAST AND DESTABILIZED CR-MN WHITE CAST IRONS

I. Chakrabarty

Banaras Hindu University, Varanasi, India

Copyright © 2011 American Foundry Society

### Abstract

*The effect of the addition of copper to Cr-Mn white cast irons in the as-cast and destabilized conditions and their performance in the chloride corrosive media were studied. This research was part of the development programme to consider substitute alloys for the existing costly wear resistant alloys like Ni-Cr or High Cr white cast irons for wear resistant applications. In the as-cast condition, a predominantly austenitic matrix was developed by the addition of Mn (~5%) and Cu (~3%) to the base iron with 2.8%C, 1.7%Si, and 6%Cr. These metastable austenitic alloys were subjected to destabilization ausaging treatment. The corresponding transformation behavior was*

*characterized by optical microscopy, hardness measurement, x-ray diffraction analysis, and electron probe micro-analysis etc. The corrosion rate in 5% NaCl aqueous solution were measured by potentiostatic method and the corroded surfaces were examined under a scanning electron microscope with EDX facility. The observations prove the beneficial effect of copper on increasing the corrosion resistance of Cr-Mn white cast irons.*

**Keywords:** corrosion resistance, ausaging, corrosion-erosion, slurry media

### Introduction

Conventional alloyed white cast irons used for wear resistant applications are mostly either high chromium or nickel-chromium white cast irons. However, there has been a continuing interest in the development of substitute alloy irons to provide either a partial or total replacement of costly and scarce alloying elements like Ni, Mo etc. in the aforesaid alloys. Manganese, a comparatively cheaper alloying element, has been used to replace the more expensive elements in alloys like Ni-hard type irons.<sup>1-4</sup> The pearlitic transformation in chromium cast irons can be successfully suppressed by the addition of manganese.<sup>5</sup> Because of its strong austenite stabilizing characteristics, the manganese percentage is restricted in as-cast martensitic irons. However, the austenite in the matrix can be subsequently reduced by a suitable destabilization treatment which would transform the retained austenite into martensite embedded with fine secondary carbides. The work hardening characteristics of the high manganese austenitic irons have also been reported to result in the high wear resistance during impact-abrasive wear.<sup>6</sup> The alloy cast iron with an austenitic matrix perform well in impact-wear applications.<sup>4,7,8</sup> Many cast iron components employed in mining and farm machinery, slurry pumps etc. are subjected not only to wear but also to corrosion in aggressive environments. In this respect, the addition of copper to Cr-Mn white cast irons appears to be beneficial because it partitions mainly to the austenitic phase<sup>5</sup> and enhances resistance to aqueous corrosion.<sup>9-11</sup> The aim of this article is to study the effect of the addition of copper to the as-cast and

heat treated microstructure and the corresponding electrochemical corrosion behavior of Cr-Mn white cast irons.

### Experimental

The alloys were made in a basic lined 4kg. indirect arc furnace from white cast iron foundry returns and ferroalloys. Electrolytic grade copper strips were used for the addition of copper. Cylindrical test bars (2cm. diameter and 15cm. long) were cast in resin bonded sand molds at 1500C (2732F). Table 1 shows the composition of the alloys cast and the percentages of retained austenite content in as-cast condition. The retained austenite contents were measured by x-ray diffraction analysis using Mo K $\alpha$  radiation.

The alloys were subjected to destabilization or ausaging treatments to destabilize the austenite in the as-cast matrix. The ausaging treatment involves aging at the lowest possible temperature in the  $\gamma$ + carbide phase field (just above A<sub>3</sub> temperature) of the alloy, followed by air cooling to room temperature. The equilibrium austenite at this lowest possible temperature has minimum solid solubility for carbon and other alloying elements. So, during aging treatment at this temperature, the excess alloying elements diffuse out of the alloy saturated austenite matrix in the form of fine secondary alloy carbides. The primary eutectic carbides are formed during eutectic solidification. Consequently, the martensite start (Ms) temperature is raised above room temperature and with the corresponding critical cooling rate still remaining low, the alloy depleted austenite will transform to martensite during subsequent cooling to room

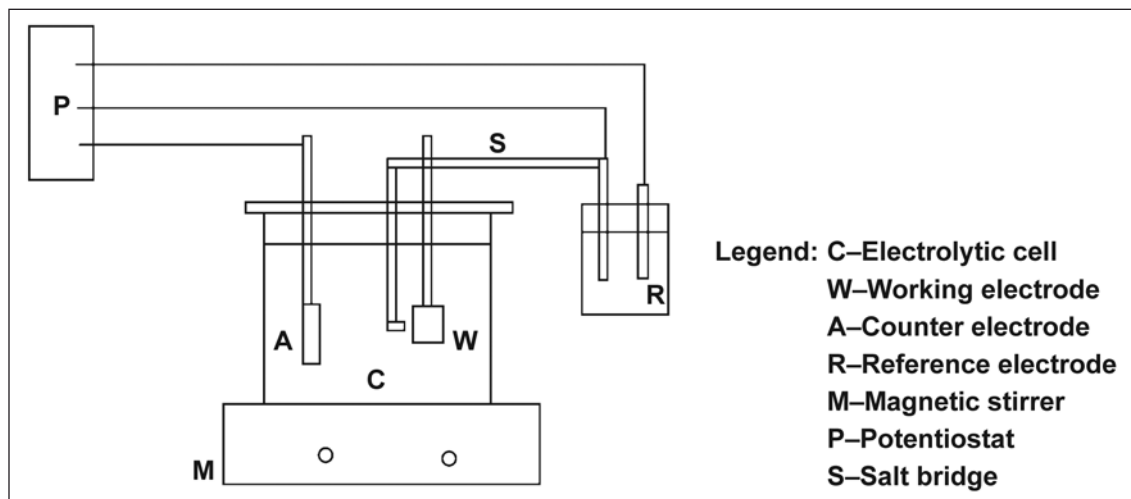


Figure 1. Schematic diagram of experimental set-up for potentiostatic polarization measurements.

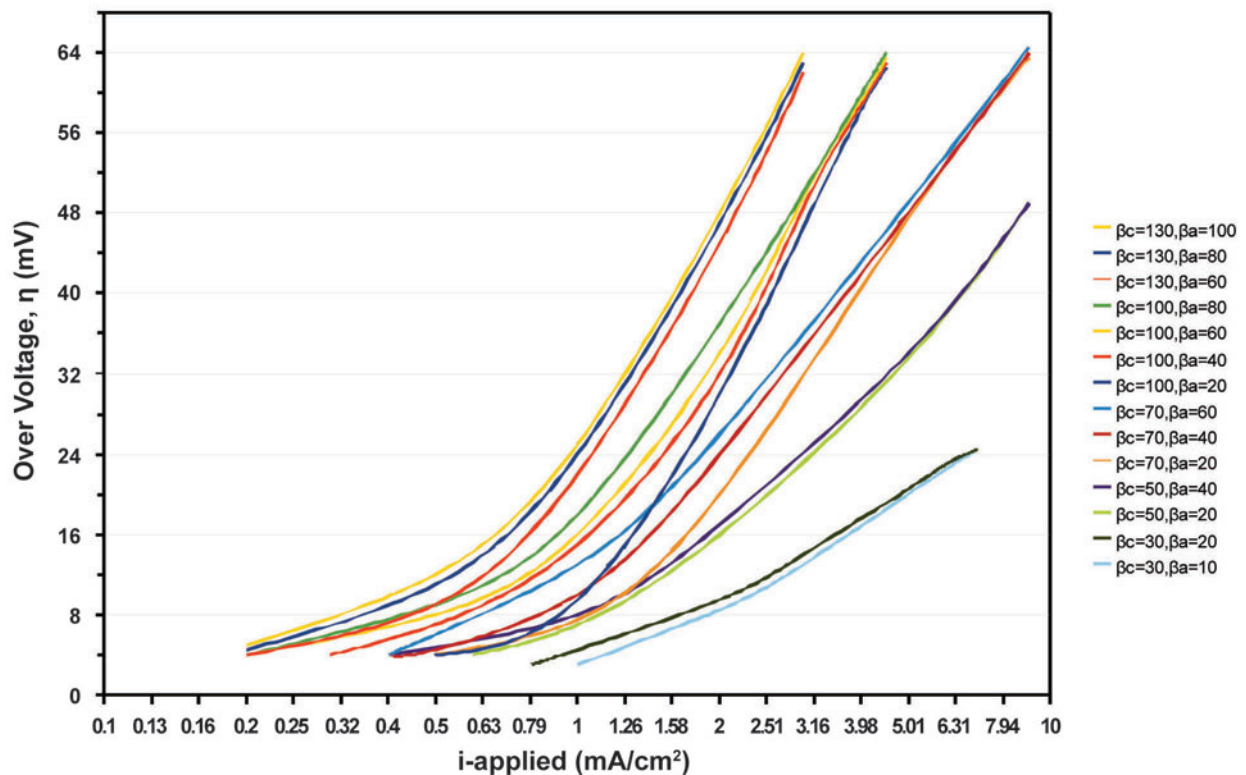


Figure 2. Plots of  $i_{applied}$  vs.  $\eta$  for various combinations of  $\beta_c$  and  $\beta_a$  and  $i_{corr} = 1.0 \text{ MA/cm}^2$

Table 1. Compositions, Hardness and Percent Retained Austenite of the As-Cast Alloys

Alloy No.	%C	%Si	%Cr	%Mn	%Cu	%Ni	Hardness (HRC)	% Retained Austenite
330	2.76	1.76	5.62	4.68	-	-	50	17.37
333	2.81	1.75	5.78	4.80	2.85	-	48	74.81
Ni-4	2.9	1.85	9.2	-	-	5.6	53	55.20

temperature. To select the critical temperature for ausaging, the as-cast alloy 333 was tempered isochronally for a fixed time of one hour at temperatures of 600,700,800 and 900C (1112, 1292, 1472 and 1652F respectively) followed by air cooling. The effect of aging time was then studied at the optimum temperature selected from the isochronal treatment results.

The matrix and the carbide morphology in the as-cast and heat treated conditions were examined by optical microscopy. The bulk hardness and the matrix hardness were measured in HRC and HV(0.1) scales respectively. The distribution of elements Si, Cr, Mn and Cu in the microstructure of ausaged sample were analyzed by electron probe micro-analysis (EPMA) in a Jeol-Superprobe 733 analyzer.

The corrosion rate was measured using the cathodic polarization method with as-cast and destabilized alloys with and without copper. For comparison purposes, the corrosion rate of a standard nickel-chromium alloy (Ni-hard type IV) was also tested. The experimental set-up is shown schematically in Fig. 1. The electrolytic cell (C) consists of a 5% NaCl solution in a glass beaker. The working electrode (W) i.e., the alloy of which the corrosion rate is to be measured and the counter electrode (A) were introduced into the cell. The counter electrode was a flat platinum foil of 4cm.x 4cm. in size. The Luggin capillary probe (S) that sensed the potential of the working electrode, contained saturated KCl in agar agar, and was connected to the reference electrode and the counter electrode through a 'Wenking' Potentiostat type 70TS1.

The specimen used for the polarization study were cylindrical in shape (1cm. diameter x 5cm. length) and were coated with cold setting resin except for one of its cross-sectional sides. This bare surface was polished and cleaned with alcohol and dried. The specimen and the counter electrode were placed into the electrochemical cell and were pre-exposed to the test solution for a sufficient length of time to attain a steady state potential and the same was noted. The cathodic polarization was then initiated from the steady state potential. The current density and the corresponding potential were measured. The corrosion current ( $i_{corr}$ ) and Tafel constants ( $\beta_c$  and  $\beta_a$ ) were measured by a nomogram<sup>12</sup> of overvoltage ( $\eta$ ) vs. ' $i_{applied}$ ' using

different sets of  $\beta_c$  and  $\beta_a$  values. The  $i_{corr}$  is fixed at 1mA/cm<sup>2</sup>. The nomogram is shown in Fig. 2. The following steps were adopted for determination of the system parameters:

- The overvoltage ( $\eta$ ) vs. current density curves were plotted using the same overvoltage scale as used in the nomogram.
- The nomogram was placed onto the graph so that the two axes coincided with those of the nomogram.
- The best fit curve was selected on the nomogram with which the experimental curve matched by sliding the nomogram along the x-axis on both sides of the origin. The  $\beta_c$  and  $\beta_a$  values corresponding to the selected curve were noted. The current value of the experimental curve which matched with the current value of 1mA/cm<sup>2</sup> of the nomogram is the required  $i_{corr}$  value.

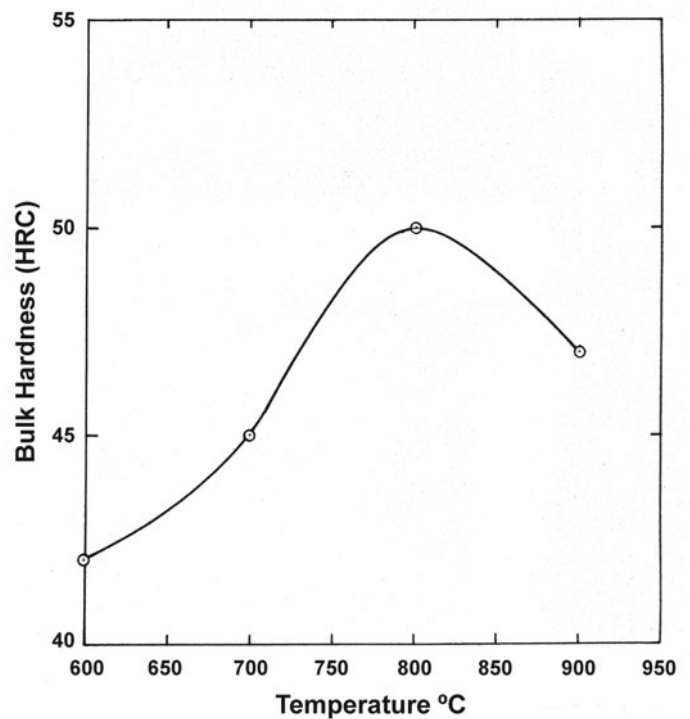


Figure 3. Bulk hardness vs. isochronal treatment temperature plot for as-cast alloy 333.

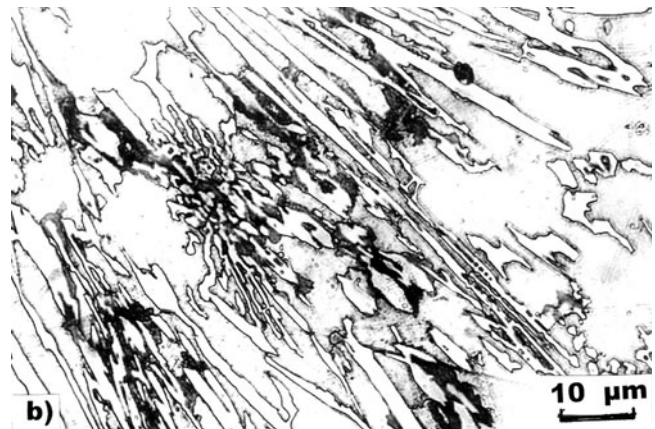
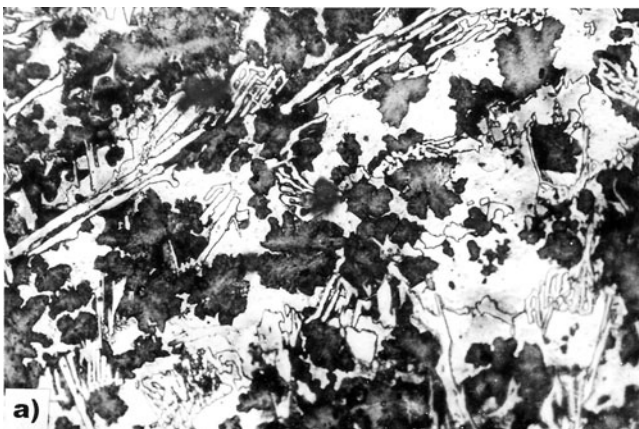


Figure 4. Optical micrographs of alloys; a) as-cast alloy 330 (without copper) and b) as-cast alloy 333 (with copper).

For examination of the characteristics of the surface corroded in saline media, the samples were kept immersed in an aqueous solution of 5% NaCl for 15 days and the surfaces were examined under a 'Camscan' scanning electron microscope with EDX facility.

## Results & Discussion

### A) Phase Transformation Behavior:

The selection of the ausaging temperature is very critical because the structural evolution in the alloy depends on this aging temperature. Figure 3 indicates that the bulk hardness of alloy 333 reaches its maximum when the sample is tempered isochronally at 800C (1472F) for one hour.

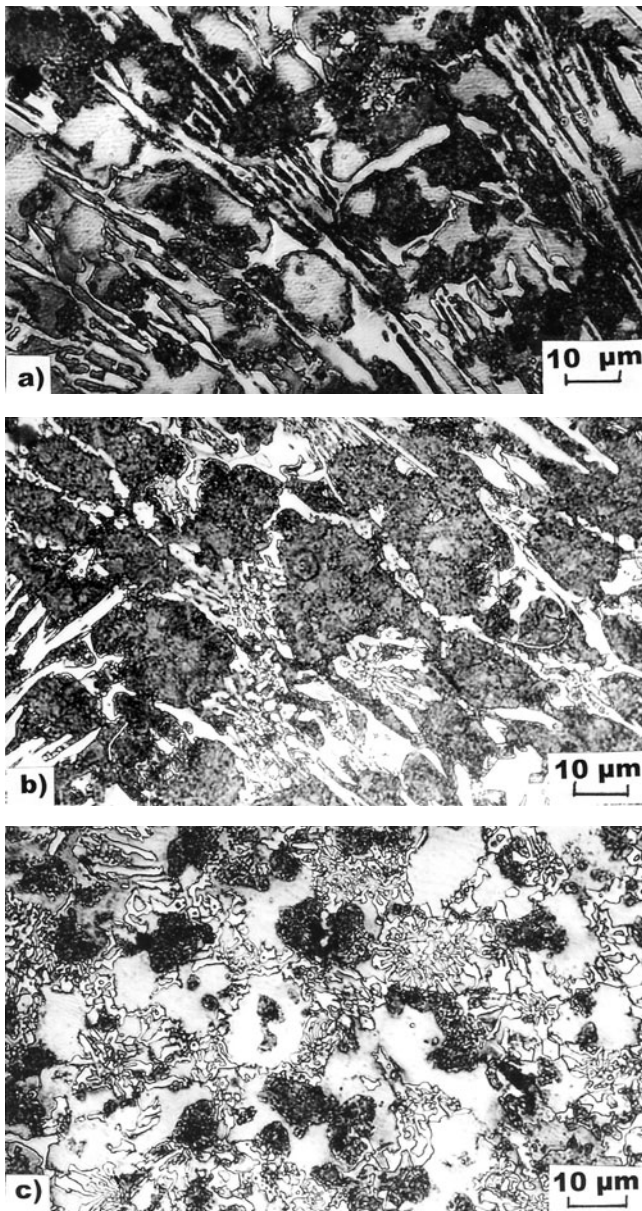


Figure 5. Optical micrographs of alloy 333, treated for 1 hour at: a) 700C (1292F), b) 800C (1472F) and c) 900C (1652F).

The corresponding optical micrograph (Fig. 5b) reveals that the austenitic matrix (Fig. 4b) gets totally transformed into martensite embedded with fine precipitates of carbides. While at 700C (1292F), a few patches of untransformed austenite are observed (Fig. 5a). The ausaging temperature of 900C (1652F) is perhaps too high above the  $A_3$  temperature of the alloy, because the austenite phase becomes stabilized again as revealed by the optical micrograph (Fig. 5c). Due to the presence of retained austenite as well as coarsening of carbide precipitates, the hardness falls. Thus, the ausaging temperature 800C (1472F) appears to be optimum.

The variation of ausaged hardness (HRC) with ausaging time at 800C (1472F) have been exhibited in Figure 6. After

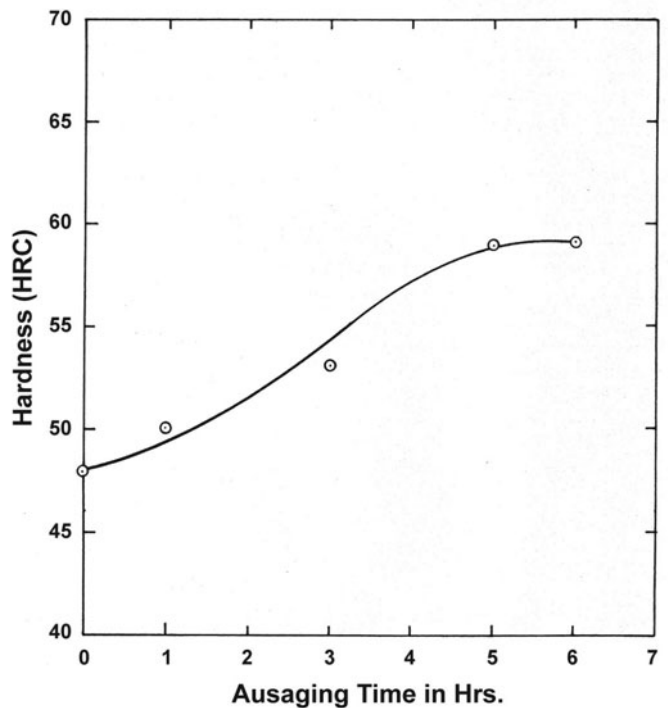


Figure 6. Hardness vs. ausaging time curve at 800C (1472F) for alloy 333.

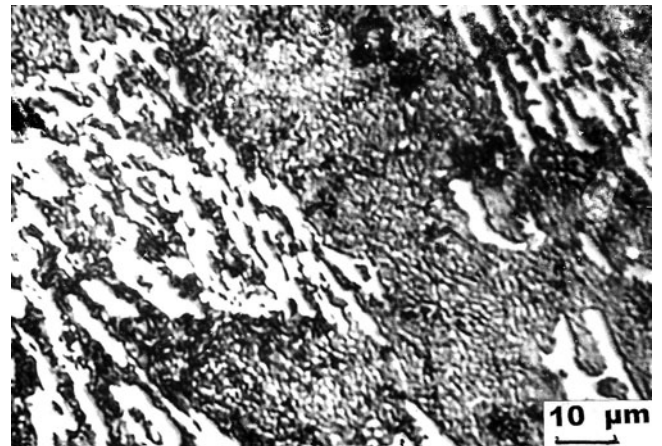
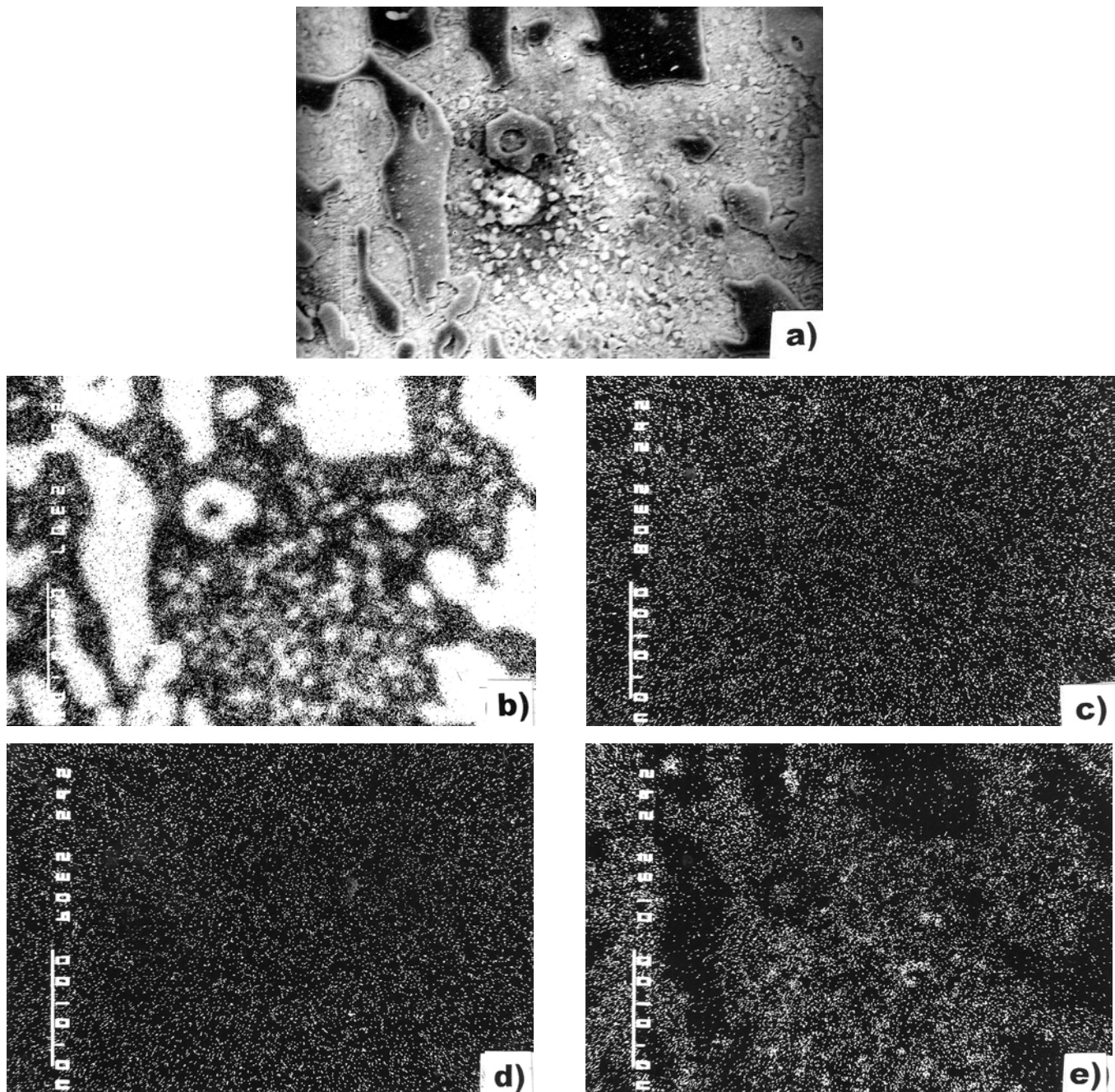


Figure 7. Optical micrograph of ausaged alloy 333 (5hrs. at 800C [1472F]).

6 hours of aging, hardness values in the range of 57-59 HRC are developed in alloys 330 and 333. With the progress of aging at the optimum temperature, the austenitic matrix gets transformed into a dark matrix embedded with fine and uniformly dispersed globular carbides (Fig. 7).

On aging near the  $A_3$  temperature, two types of reactions may occur according to the aging temperature selected. At temperatures higher than the  $A_3$  temperature, the carbide precipitation does not provoke any allotropic transformation during aging and the austenitic matrix is merely depleted of

carbon and other alloying elements, due to the precipitation of carbides. The reaction can be written as  $\gamma \rightarrow \gamma_1 + \text{carbides}$ , where  $\gamma_1$  is alloy depleted austenite. At temperatures below the  $A_3$  temperature, the carbide precipitation is accompanied by a partial transformation of austenite into pearlite or ferrite-carbide aggregate. The reaction can be written as  $\gamma \rightarrow \gamma_1 + (\alpha + \text{carbides})$  where  $\alpha$  is ferrite. The electrolytically extracted carbides from the ausaged samples when subjected to x-ray diffraction analysis, are identified mostly as chromium carbides of  $M_7C_3$  types. The x-ray mappings for the alloying elements present (Cr, Mn, Si, and Cu) obtained by EPMA in



**Figure 8.** SEM image and corresponding x-ray map of ausaged alloy 333: a) SEM micrograph, b) Cr K $\alpha$  x-ray map, c) Mn K $\alpha$  x-ray map, d) Si K $\alpha$  x-ray map and e) Cu K $\alpha$  x-ray map.

the ausaged alloy 333 are shown in Figure 8. Chromium is found to be distributed in primary as well as secondary carbides and copper in the matrix. But copper distribution in the matrix is not homogeneous. As the solid solubility of copper is poor, except in austenite, it will precipitate out from the transformed austenite phase.<sup>13</sup> Manganese and silicon are present both in carbides and the matrix.

### B) Corrosion Behavior:

The corrosion rate measurements using the cathodic polarization method were carried out on alloys 330, 333 and Ni-hard alloy for comparison and a typical overvoltage versus current density plot for as-cast alloy 333 is shown in Figure 9. The important electrochemical parameters obtained are shown in Table 2.

The analysis of the polarization data indicates that amongst the alloys studied, the alloy 333 in as-cast condition has a minimum corrosion current and the same is comparable to that of nickel-chromium iron (type IV). However, in ausaged condition the same alloy shows an increased rate of corrosion. The copper free chromium-manganese ausaged alloy 330 with almost the same microstructure as the ausaged alloy 333, indicates a considerable increase in corrosion rate. These observations indeed prove the beneficial effect of copper on increasing the corrosion resistance. The alloy 333 in ausaged condition with a large number of precipitates in the matrix, exhibits a decreased corrosion resistance than the as-cast predominantly austenitic alloy of the same composition. This is due to local cell formation in a chloride solution with the secondary carbides as cathode and the matrix as anode. This is evident in the corroded SEM micrographs (Fig. 10).

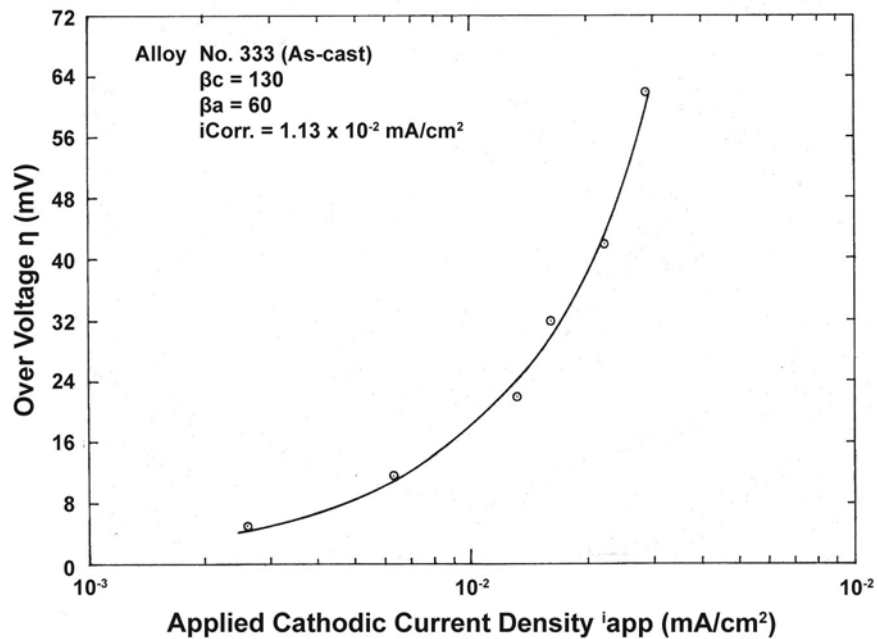


Figure 9. Cathodic polarization curve for as-cast alloy 333 in 5% NaCl solution.

Table 2. Electrochemical Parameters of Cathodic Polarization

Alloy No.	Condition	Cathodic Slope( $\beta_c$ )	Anodic Slope ( $\beta_a$ )	Corrosion Current ( $i_{corr}$ ),mA/cm <sup>2</sup>
330	Ausaged at 800C (1472F) + 5hrs.	130	60	$2.55 \times 10^{-2}$
333	Ausaged at 800C (1472F) + 6hrs	130	100	$1.95 \times 10^{-2}$
333	As-cast	130	60	$1.13 \times 10^{-2}$
Ni-4	Ausaged	100	60	$1.30 \times 10^{-2}$

A single phase microstructure with a close packed crystal structure is most useful in resisting corrosion. Presence of a passive film would be an added advantage. In chromium cast irons, an adherent and impervious layer of chromium oxide is formed on the surface. Due to this, chrome irons are resistant to the action of different corroding media.<sup>14,15</sup> Copper appears to act in the same way as chromium in the formation of a protective layer. This is substantiated by the EDX analysis which shows an enrichment of copper at the surface. Similar findings were reported by Szpunar<sup>16</sup> on the effect of copper on corrosion resistance of Ni-Mn-Cu cast iron in chloride solution. According to Szpunar, the layer nearest to the metal surface contains  $Fe_3O_4$ ,  $Fe_2O_3$ ,  $CuO$  as revealed by electron diffraction analysis.

### Conclusions

- Addition of copper increases the corrosion resistance of Cr-Mn white cast irons in chloride medium.
- The best corrosion resistance property is obtained with a predominantly austenitic matrix.
- The corrosion rate increases when the austenitic matrix is destabilized by an ausaging treatment. This is due to the formation of fine secondary car-

bides in the matrix which are acting as cathode and the matrix as anode in the chloride media.

- The increase in corrosion resistance property by copper addition is perhaps due to the formation of an adherent and impervious protective layer of copper oxide on to the surface of Cr-Mn irons.

### REFERENCES

1. Levi, L.I. et.al., "Wear-Resistant Chromium-Manganese Cast Iron," *Russian Casting Production*, pp. 409-412 (August 1967).
2. Basak, A., Penning, J., & Dilewijns, J., "Effect of Manganese on Wear Resistance and Impact Strength of 12% Chromium White Cast Iron," *International Cast Metals Journal*, vol. 6, no. 3, pp.12-17 (Sept. 1981).
3. Basak, A., Penning, J., & Dilewijns, J., *Metals Technology*, vol. 9, no. 9, p.381 (Sept. 1982).
4. Chakrabarty, I. & Basak, A., "Aus-Aging" and Corrosive Wear Behavior of Cr-Mn-Cu White Cast Irons," *AFS Transactions*, vol. 98, p. 707 (1990).
5. ASM Metals Handbook; 9<sup>th</sup> Edition, vol.1, Properties and Selection: Irons and Steels, p.75 and p.597 (1978).
6. Cox, G.J., "Developments in Alloy Cast Irons," *The*

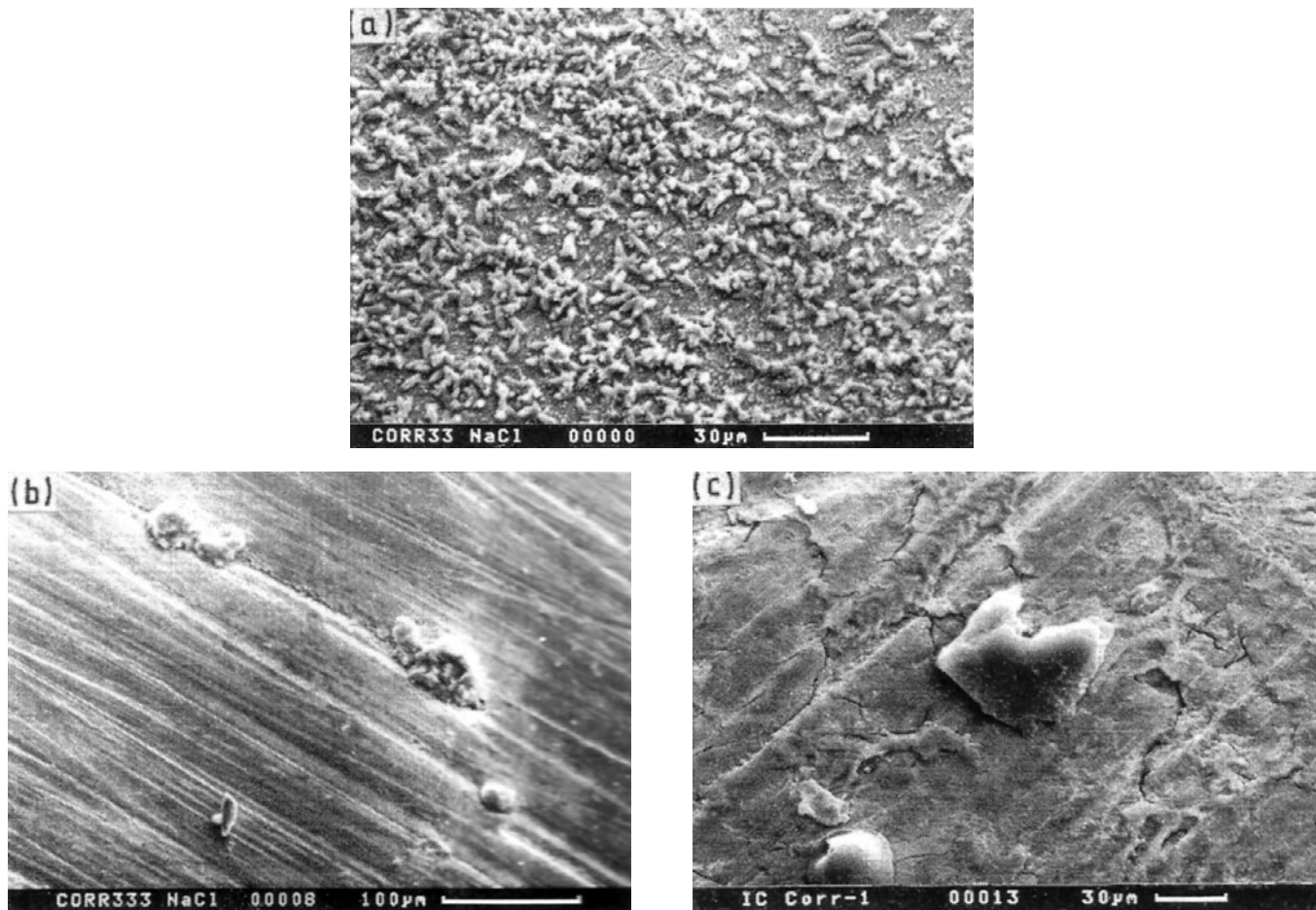


Figure 10. SEM micrographs of the corroded surface in 5% NaCl solution: a) alloy 330 ausaged, b) alloy 333 ausaged and c) Ni- hard alloy IV ausaged.

- British Foundryman*, vol. 76, p.129 (1983).
7. Jackson, R.S., "Metallurgical and Production Aspects of High Chromium Cast Irons for Abrasion Resisting Applications," *The British Foundryman*, vol. 67, p. 34 (1974).
  8. Durman, R.W., "The Application of Alloyed White Cast Irons in Crushing, Grinding, and Material Handling Processes," *The British Foundryman*, vol. 69, p.141 (1976).
  9. Pearce, J.G. & Bromage, K., *Copper in Cast Iron*, p. 61, Copper Development Association Publication, London (1964).
  10. Prasada Rao, P.N.V.R.S.S.V., Patwardhan, A.K. & Jain, N.C., "Effect of Microstructure on the Corrosion and Deformation Behavior of a Newly Developed 6Mn-5Cr-1.5Cu Corrosion-Resistant White Iron," *Metallurgical and Materials Transactions A*, vol. 24, no. 2, pp. 445-457 (Feb.1993).
  11. Patwardhan, A.K. & Jain, N.C., "Modeling of the Corrosion Behavior and Its Interrelation with the Deformation Behavior and Microstructure in a Newly Developed 7.5Mn-5Cr-1.5Cu Alloy White Iron," *Metallurgical and Materials Transactions A*, vol. 22, no. 10, pp. 2319-2325 (Oct.1991).
  12. Chakrabarty, I., Ph.D. Thesis, I.I.T, Kharagpur (1988).
  13. Kumar, V., "Formation and Morphology of M7C3 in Low Cr White Iron Alloyed with Mn and Cu," *Journal of Materials Engineering & Performance*, vol.12, no. 1, pp. 14-18 (Feb. 2003).
  14. Neville, A., Reza, F., Chiovelli S., & Revega, T., "Characterization and Corrosion Behavior of High-Chromium White Cast Irons," *Metallurgical and Materials Transactions A*, vol. 37, no. 8, pp. 2339-2347 (Aug.,2006).
  15. Zumelzu, E., Goyos, L., Cabezas, C., Opitz,O., Quiroz, E., & Parada A., "Wear and Corrosion Behaviour of High-Chromium (14-30% Cr) Cast Iron Alloys," *Journal of Materials Processing Technology*, vol. 128, pp. 250-255 (Oct. 2002).
  16. Szpunar, E., *Ochrona Przed Korozja*, p.11 (Oct. 1970).

## Technical Review and Discussion:

### Effect of Copper on the Corrosion Resistance Behaviour of As-Cast and Destabilized Cr-Mn White Cast Irons

I. Chakrabarty, Banaras Hindu University, Varanasi, India

**Reviewer:** For commercial utilization, a comparison to higher Cr irons needs to be included.

**Author:** Commercial Nickel-chromium alloy (Ni-hard , grade 4) was chosen as a standard sample to compare

the performance with the experimental alloys in chloride media. Unfortunately, I am unable to furnish the comparative data of commercial high chromium irons with my own experimental condition. However, I have collected some data from literature\* on the 'Icorr' values of different grades of high Cr-irons in 1000 ppm NaCl solution with pH 8.

\*A.Neville, F.Reza, S.Chiovelli and T.Revega; "Characterization and Corrosion behavior of high chromium white cast irons, *Metallurgical & Materials Transaction A*, Vol.37A, August 2006, p.2339.

